Density-Tuned Polyolefin Phase Equilibria. 2. Multicomponent Solutions of Alternating Poly(ethylene–propylene) in Subcritical and Supercritical Olefins. Experiment and SAFT Model

Shean-Jer Chen,† Ioannis G. Economou,†,‡ and Maciej Radosz*,†

Corporate Research, Exxon Research & Engineering Company, Annandale, New Jersey 08801, and Department of Chemical Engineering, The Johns Hopkins University, Baltimore, Maryland 21218

Received December 2, 1991; Revised Manuscript Received May 11, 1992

ABSTRACT: Different phase transitions (LCST, UCST, VL, and VLL) in binary, ternary, and, quaternary olefin–polyolefin systems are found to be easily tuned with density. Polyolefin is alternating poly(ethylene–propylene), PEP for short. The PEP phase transitions are quantitatively related to pressure, temperature, solvent composition, and its size. For example, supercritical ethylene drastically reduces the mutual solubilities of comonomers and PEP and hence increases the minimum pressure needed for complete miscibility. This ethylene antisolvent effect is modeled with statistical associating fluid theory (SAFT). SAFT also predicts that LCST and UCST curves can merge into a single U-LCST curve upon increasing the size difference between the polymer and solvent. Furthermore, one internally consistent set of SAFT parameters can correlate LCST, VL, and VLL equilibria simultaneously, which has not been demonstrated before. SAFT is verified experimentally with new phase equilibrium data obtained in an optical variable-volume cell for ternary PEP solutions in propylene + ethylene, 1-butene + ethylene, and 1-hexene + ethylene.

1. Introduction

Polymer solution phase behavior strongly depends on both free-volume and energetic contributions of the constituent components. As temperature increases, especially near the solvent critical point, polymer solutions exhibit liquid–liquid immiscibility that is due mainly to large differences in "free volume" between the polymer molecules and the solvent molecules.[1] This type of phase transition is often referred to as the LCST-type (lower critical solution temperature). As temperature decreases, on the other hand, polymer solutions exhibit a different region of limited miscibility that is referred to as the UCST-type (upper critical solution temperature[1,2]), which is due mainly to large differences in interaction energies between the polymer and solvent molecules. For temperatures between the UCST and LCST the system is miscible for all compositions. For associating systems, specific interactions (such as hydrogen bonding) will significantly affect phase behavior.[3,4]

The UCST- and LCST-type phase behaviors of polymer solutions have been examined experimentally by many investigators. Examples include polyisobutylene in alkanes,[5] polystyrene in various solvents,[6–13] and polyethylene in ethylene.[14,15] In cross-associating systems, such as poly(ethylene glycol) in water, closed-loop phase diagrams have been found[13] and attributed to hydrogen bonding. In all these systems, the polymer molecular weight and system pressure have an appreciable effect on the phase behavior. These two effects are the focus of an experimental study by Chen and Radosz,[16] who report phase equilibrium data for binary solutions of narrow distributed poly(ethylene–propylene) in propylene, 1-butene, and 1-hexene.

In the last decade, the use of supercritical fluids (SCFs) as antisolvents in polymer solutions has attracted considerable attention. Addition of a supercritical solvent to a liquid solution can lower the LCST by more than 100 °C[17] and hence precipitate the polymer from its original solution. Examples of SCFs are ethane, ethylene, and carbon dioxide.[17–19] The use of SCFs as antisolvents is described by McHugh and Krukonis.[20]

From among theoretical models proposed to describe the phase behavior of polymer systems, the most widely known is the Flory–Huggins lattice theory[21] that was later modified by Patterson and co-workers.[5,9] The original rigid lattice theory by Flory does not account for LCST demixing. Chen and Radosz[16] used the Patterson expression for χ coupled with the Flory theory to reproduce experimental LCST curves for binary polyolefin + olefin systems. Recently, Qian et al.[22] generalized different kinds of phase diagrams for polymer solutions and blends by making Flory's χ parameter composition- and temperature-dependent. Flory et al.[23] proposed an equation of state (FOV equation of state) that is extensively used for polymer systems.[24,25] Other equations of state used for polymers are perturbed-hard-chain-theory (PHCT)[26,27] and Sanchez–Lacombe.[4,19,28] The difficulty with using these equations of state stems from how to determine the polymer parameters and how to relate them to molecular size and structure distribution.

One goal of this work is to determine experimentally the phase behavior of alternating poly(ethylene–propylene) (PEP) fractions that have very uniform structure and very narrow molecular weight distributions, in solutions with 1-butene–ethylene and 1-hexene–ethylene, at a constant polymer concentration of about 15 wt %. Another goal of this paper is to model the experimental data obtained in this work, as well as the binary data reported by Chen and Radosz,[16] using the statistical associating fluid theory (SAFT). SAFT is an equation of state for small and large, associating and nonassociating molecules developed by Chapman et al.[29] and Huang and Radosz.[30,31] The advantage of SAFT is that the pure-component parameters for polyolefins can be determined from generalized correlations on the basis of their molecular weights.

SAFT is applicable to chainlike molecules, such as polymers, because it has a chain term rigorously derived on the basis of statistical mechanics. This chain term, for example, allows SAFT to capture the compressibility factor

* Author to whom correspondence should be addressed.
† Exxon Research & Engineering Company.
‡ The Johns Hopkins University.

0024-9297/92/2225-4987$03.00/0

Table I
Poly(ethylene–propylene) Materials Used in This Work[a]

sample	M_w	M_w/M_n	sample	M_w	M_w/M_n
PEP790	790	1.01	PEP26k	26 000	1.03
PEP5.9k	5 900	1.08	PEP96k	96 400	<1.1

[a] M_w is the weight-average molecular weight, and M_w/M_n is the polydispersity index.

data obtained from Monte Carlo (MC) simulations on hard-sphere chains. This was demonstrated by Chapman et al.,[29] who found that SAFT is in excellent agreement with the available (up to 16 segments) MC data. SAFT molecules are modeled as effective chains of freely jointed spheres. Hence, SAFT chains are flexible, and not rigid, because in SAFT we do not specify bond angles or bonding site locations.

2. Experimental Section

Phase boundaries are measured in a batch optical cell equipped with a sapphire window and movable piston. The piston controls volume, and hence pressure, at constant composition and temperature. The maximum volume is 17 cm^3. Phase transitions are observed visually, typically in the form of a cloud-point transition, by displaying the window image, via a borescope, on a video screen. Detailed description of the equipment and procedure for binary systems is provided by Chen and Radosz.[16] Here is a brief overview of the procedure used in this work for ternary systems.

The known amounts of polymers (from weighing) and condensable solvents (from reading a syringe pump scale) are loaded into the cell. Ethylene, on the other hand, is added to the cell through one of the three sampling lines (top) from a miniature sample cylinder (Whitey Co. Model SS-4CS-TW-10). The amount of ethylene added to the cell is obtained from weighing. The amount of ethylene left in the sampling line and the valve is tested to be negligible; the valve has no dead volume, and the short sampling line has an inside diameter of only 0.025 cm.

After allowing sufficient time for polymer swelling, the solution is brought into a one-phase region by increasing the pressure while stirring. Then, the pressure is lowered slowly until the mixture starts becoming cloudy. This indicates the onset of phase separation. The corresponding pressure is recorded as the cloud-point pressure. The pressure is further reduced to observe phase disengagement patterns. In addition to one-to-two and two-to-three phase boundaries, we observe two different patterns of phase disengagement. One pattern is referred to as a bubble-point-like transition, where one observes the onset and growth of the low-density phase upon lowering the pressure. Another pattern is referred to as a dew-point-like transition, where one observes the onset and growth of the high-density phase upon lowering the pressure.

Mixture compositions are obtained either from the known amount of each component (synthetic method) or from the material balance based on volumetric–gravimetric sampling and subsequent GC or mass spectrometry analysis (analytic method). The compositions of 1-hexene solutions are determined from the synthetic method, while the compositions of 1-butene and propylene solutions are determined from the analytic method.

Poly(ethylene–propylene) materials (PEPs) used in this work were prepared by quantitative hydrogenation of polyisoprenes obtained from anionic synthesis by Fetters, as described by Mays et al.[32] The weight-average molecular weights (M_w) by light scattering and the polydispersity indices (weight-to-number ratios, M_w/M_n) by SEC are given in Table I. The other, purchased commercially materials are reagent grade with a minimum purity of 99%.

3. Statistical Associating Fluid Theory (SAFT)

SAFT is an equation of state that explicitly accounts for nonspecific (repulsive, dispersion) and specific (association due to hydrogen bonding) interactions among molecules. In a simplified physical picture, a pure SAFT fluid is a collection of equisized hard-spherical segments that not only are exposed to mean-field (dispersion) forces but also (a) can be covalently bonded to form chain molecules and (b) can be weakly (e.g., hydrogen) bonded to form short-lived clusters. Both covalent and hydrogen bond energies are modeled with square-well potentials. Such a SAFT fluid model captures key features of real molecules, from small, near-spherical, and nonassociating to large, strongly nonspherical, and strongly associating.

While rooted in cluster expansion perturbation theory proposed by Wertheim[33-35] for hard spheres with off-center attractive sites, SAFT has been extended to real molecules, macromolecules,[29,30] and mixtures.[31] As a result, as described in detail by Huang and Radosz,[30] the reference part of SAFT consists of hard-sphere, chain, and association terms whereas the perturbation part is a relatively weaker mean-field (dispersion) term. The residual Helmholtz free energy is given by

$$a^{res} = a^{ref} + a^{disp} \tag{1}$$

where the reference term is a sum of the hard-sphere, chain, and association contributions

$$a^{ref} = a^{hs} + a^{chain} + a^{assoc} \tag{2}$$

Since the systems examined in this work do not exhibit specific interactions that can lead to association, we set a^{assoc} in eq 2 equal to zero. The hard-sphere term for pure components is calculated from the Carnahan and Starling[36] equation

$$\frac{a^{hs}}{RT} = m\frac{4\eta - 3\eta^2}{(1-\eta)^2} \tag{3}$$

where m is the number of segments per molecule and η is the reduced density. Equation 3 is extended to mixtures by Huang and Radosz[31] on the basis of statistical mechanical arguments proposed by Mansoori et al.[37] The chain term is given by

$$\frac{a^{chain}}{RT} = (1-m)\ln g^{hs} \tag{4}$$

where g^{hs} is the contact value of the radial distribution function given by Carnahan and Starling[36] for the hard-sphere fluid

$$g^{hs} = \frac{2-\eta}{2(1-\eta)^3} \tag{5}$$

Similar to eq 3, eq 4 is extended to mixtures on the basis of statistical mechanics as described by Huang and Radosz.[31] This way the whole reference part of SAFT (a^{ref}) has been extended to mixtures on the basis of rigorous statistical mechanics, without having to invoke mixing rules. Only the minor dispersion part a^{disp} has been extended to mixtures using several types of mixing rules, as described by Huang and Radosz[31]. The dispersion part of SAFT is a power series in temperature and density, which was initially fitted to molecular dynamics data for a square-well fluid by Alder et al.[38]

$$\frac{a^{disp}}{RT} = m\sum_{i=1}^{4}\sum_{j=1}^{9} D_{ij}\left(\frac{u}{kT}\right)^i\left(\frac{\eta}{\tau}\right)^j \tag{6}$$

D_{ij}s are 24 nonzero universal constants determined by Chen and Kreglewski.[39] u/k is the segment energy which is a temperature-dependent characteristic parameter in the equation of state[30] and $\tau = 0.7405$. In order to extend eq 6 to mixtures, we use the van der Waals one-fluid theory

(vdW1) mixing rules as

$$\frac{u}{kT} = \frac{\sum_i \sum_j X_i X_j m_i m_j \left(\frac{u_{ij}}{kT}\right)(v^\circ)_{ij}}{\sum_i \sum_j X_i X_j m_i m_j (v^\circ)_{ij}} \tag{7}$$

where

$$(v^\circ)_{ij} = \left[\frac{1}{2}[(v^\circ)_i^{1/3} + (v^\circ)_j^{1/3}]\right]^3 \tag{8}$$

$$u_{ij} = (u_{ii}u_{jj})^{1/2}(1 - k_{ij}) \tag{9}$$

$$m = \sum_i \sum_j X_i X_j m_{ij} \tag{10}$$

$$m_{ij} = \frac{1}{2}(m_i + m_j) \tag{11}$$

X_i is the mole fraction of component i, and v° is the temperature-dependent segment volume. In summary, we model real molecules as effective chains and characterize them with three molecular parameters; segment number (m, number of segments in each molecule), segment volume (temperature-independent, $v^{\circ\circ}$ in mL/mol of segments), and temperature-independent segment energy (u°/k in kelvin). The relationships between the temperature-independent $v^{\circ\circ}$ and the temperature-dependent v°, on the one hand, and the temperature-independent u°/k and temperature-dependent u/k, on the other hand, are given by Huang and Radosz.[30] For mixture calculations, one binary adjustable parameter, k_{ij}, is needed that is fitted to phase equilibrium data or estimated from empirical correlations presented in this paper.

The molecular parameters are determined by fitting the equation of state to experimental vapor pressure and saturated liquid density data.[30] This procedure is successful for small molecules but is not applicable to large polymeric molecules that have very low vapor pressure (practically zero). For polymers, the equation of state is usually fitted to low- and high-pressure P–V–T data in order to determine the molecular parameters.[27] SAFT parameters have been determined for a few polyolefins.[30] Since the equation of state and the molecular parameters are normalized on a per-segment basis, rather than on a molecular basis, the parameter values can be correlated against molecular weight for many compounds that are similar in structure.

We determine the equation of state parameters for polymers exclusively from such generalized correlations. For example, Huang and Radosz[30] proposed a simple empirical correlation for the segment number m for a series of n-alkanes and polyolefins, shown in Figure 1. The linear equation for m used in this work is given by

$$m = 0.05096M \tag{12}$$

where M is the molar mass in g/mol. Following Huang and Radosz,[30] we set the segment volume $v^{\circ\circ}$ equal to 12 mL/mol for all the PEP fractions and calculate the segment energy u°/k from

$$u^\circ/k = 210.0 - 26.886 \exp(-0.013341M) \tag{13}$$

which means u°/k has a constant value of 210.0 K for all the PEP fractions. All the SAFT parameters for the components used in this work, including the critical temperatures of the solvents, are shown in Table II. For the record, the molecular parameters refitted to P–V–T data

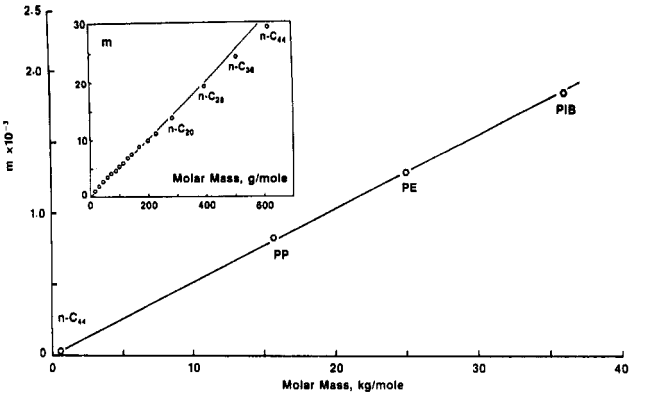

Figure 1. Segment number m in SAFT as a linear function of molar mass for n-alkanes and polyolefins: PP = polypropylene, PE = polyethylene, PIB = polyisobutene.

Table II
SAFT Molecular (Pure-Component) Parameters and Critical Temperatures for the Components Used in This Work[a]

component	T_c (°C)	m	$v^{\circ\circ}$ (mL/mol)	u°/k (K)
ethylene	9.2	1.464	18.157	212.06
propylene	91.9	2.223	15.648	213.90
1-butene	146.5	3.162	13.154	202.49
1-hexene	230.9	4.508	12.999	204.71
n-hexane	234.4	4.724	12.475	202.72
methylcyclopentane	259.6	4.142	13.201	223.25
PEP		$0.05096M_P$	12.000	210.00

[a] M_P = poly(ethylene–propylene) (PEP) molecular weight in g/mol.

obtained for the PEP samples used in this work have been tested but found to be not as reliable as those derived from the generalized correlations discussed above.

Phase equilibrium calculations are performed using an iterative algorithm based on Richmond's method.[40] In this method, an improved estimate $x^{(r+1)}$ of the root of the equation $f(x) = 0$ is calculated from a previous estimate $x^{(r)}$ as

$$x^{(r+1)} = x^{(r)} - \frac{2}{2f'(x^{(r)})/f(x^{(r)}) - f''(x^{(r)})/f'(x^{(r)})} \tag{14}$$

where prime and double prime denote the first and second derivative, respectively. We found that eq 14 converges faster than the widely used Newton–Raphson method for bubble-point calculations. All of our calculations are of the bubble-pressure type; that is, given temperature and composition of the heavy phase, we calculate the bubble pressure and the light phase composition.

4. Results and Discussion

The experimentally measured cloud-point data for 1-butene + ethylene + PEP26k and for 1-hexene + ethylene + PEP26k are reported in Table III. The experimental results are reported in a tabulated form because they provide a basis for developing thermodynamic theories and models, such as SAFT. We find it necessary to use tabulated data for such purposes, rather than rely on the data read from approximate figures. SAFT predictions, on the other hand, are shown as solid curves in plots that also show experimental points. This way one can evaluate the quality of SAFT predictions. While all these data are of the bubble-pressure-type, they represent three different types of phase transitions, such as vapor–liquid to liquid (VL), liquid–liquid to liquid (LL), and vapor–liquid–liquid to liquid–liquid (VLL).

Table III
Experimental Data for the Phase Boundaries of the Ternary Systems[a]

PEP (wt %)	ethylene (wt %)	T (°C)	P (bar)	type of equilibrium	PEP (wt %)	ethylene (wt %)	T (°C)	P (bar)	type of equilibrium
				1-Butene + Ethylene + PEP26k					
18.7	7.4	82.2	144.0	LL	16.2	11.7	125.1	266.4	LL
18.7	7.4	100.3	177.0	LL	16.2	11.7	150.0	296.8	LL
18.7	7.4	125.0	215.3	LL	16.2	11.7	174.8	322.0	LL
18.7	7.4	150.0	250.3	LL	16.2	11.7	200.3	344.5	LL
18.7	7.4	175.0	278.0	LL	15.4	23.4	82.2	318.5	LL
18.7	7.4	200.4	303.0	LL	15.4	23.4	100.4	340.2	LL
16.2	11.7	82.2	200.4	LL	15.4	23.4	125.0	365.0	LL
16.2	11.7	100.2	232.0	LL	15.4	23.4	150.1	389.0	LL
				1-Hexene + Ethylene + PEP26k					
16.0	0.0	154.0	7.2	VL	15.0	24.3	80.6	55.6	VLL
16.0	0.0	174.8	12.7	VL	15.0	24.3	98.8	63.4	VLL
16.0	0.0	194.7	17.2	VL	15.0	24.3	122.7	73.0	VLL
16.0	0.0	200.0	23.5	LL	15.0	24.3	151.0	81.2	VLL
16.0	0.0	204.8	29.4	LL	15.3	35.5	-22.0	187.0	LL
16.0	0.0	205.5	31.6	LL	15.3	35.5	-8.5	176.0	LL
16.0	0.0	200.0	19.3	VLL	15.3	35.5	-2.0	175.0	LL
16.0	0.0	204.8	20.0	VLL	15.3	35.5	9.6	182.5	LL
16.0	0.0	205.5	20.4	VLL	15.3	35.5	22.3	194.7	LL
15.8	12.2	26.5	16.9	VL	15.3	35.5	38.5	216.5	LL
15.8	12.2	50.0	23.0	VL	15.3	35.5	51.5	233.0	LL
15.8	12.2	80.3	32.1	VL	15.3	35.5	82.3	269.0	LL
15.8	12.2	100.5	38.5	VL	15.3	35.5	100.3	290.0	LL
15.8	12.2	110.9	41.2	VL	15.3	35.5	125.0	320.5	LL
15.8	12.2	124.0	44.0	VL	15.3	35.5	150.8	348.0	LL
15.8	12.2	132.6	58.0	LL	15.3	35.5	176.0	370.0	LL
15.8	12.2	140.0	68.0	LL	15.3	35.5	200.3	384.0	LL
15.8	12.2	149.0	85.0	LL	15.3	35.5	-14.3	17.2	VLL
15.8	12.2	151.6	89.2	LL	15.3	35.5	9.6	30.0	VLL
15.8	12.2	160.3	100.0	LL	15.3	35.5	22.3	36.5	VLL
15.8	12.2	174.5	124.0	LL	15.3	35.5	38.5	45.8	VLL
15.8	12.2	190.5	138.0	LL	15.3	35.5	51.5	55.0	VLL
15.8	12.2	195.4	144.0	LL	15.3	35.5	82.3	75.5	VLL
15.8	12.2	200.2	148.0	LL	15.3	35.5	100.3	85.0	VLL
15.8	12.2	151.6	53.1	VLL	15.3	35.5	125.0	91.8	VLL
15.8	12.2	160.3	54.1	VLL	14.9	50.4	22.9	488.0	LL
15.8	12.2	174.5	59.8	VLL	14.9	50.4	37.7	464.0	LL
15.8	12.2	195.0	63.2	VLL	14.9	50.4	52.6	456.0	LL
15.0	24.3	27.5	28.0	VL	14.9	50.4	70.1	452.0	LL
15.0	24.3	33.0	31.7	VL	14.9	50.4	85.7	459.0	LL
15.0	24.3	41.0	43.0	LL	14.9	50.4	101.7	468.0	LL
15.0	24.3	48.7	56.5	LL	14.9	50.4	124.1	479.0	LL
15.0	24.3	80.6	114.0	LL	14.9	50.4	151.0	492.0	LL
15.0	24.3	98.8	144.0	LL	14.9	50.4	173.4	502.0	LL
15.0	24.3	122.7	179.0	LL	14.9	50.4	196.5	511.0	LL
15.0	24.3	152.4	222.0	LL	14.9	50.4	22.5	48.6	VLL
15.0	24.3	174.7	246.0	LL	14.9	50.4	38.0	59.4	VLL
15.0	24.3	199.4	266.0	LL	14.9	50.4	52.8	70.0	VLL
15.0	24.3	42.8	35.0	VLL	14.9	50.4	70.1	79.0	VLL
15.0	24.3	50.2	39.2	VLL	14.9	50.4	85.7	88.6	VLL
15.0	24.3	68.0	47.0	VLL	14.9	50.4	101.7	92.0	VLL

[a] Ethylene composition is in polymer-free basis. VL = vapor–liquid equilibrium, LL = liquid–liquid equilibrium, VLL = vapor–liquid–liquid equilibrium. All equilibrium data are of the bubble-point type.

Like all other van der Waals-type analytical equations of state, SAFT is inaccurate in the near-critical regions. As recently illustrated for binary systems,[31] phase-boundary curves in the critical region calculated from SAFT are too highly curved; experiment says that they should be nearly flat.

The SAFT predicted values, for both binary and ternary systems, are presented as phase diagrams shown in Figures 2–13, which are two-dimensional plots of pressure (in bar) versus either temperature (in °C) or composition (in weight fractions) or PEP molecular weight. In all the figures, open data points indicate dew-point-like transitions, whereas filled data points indicate bubble-point-like transitions. The following discussion is organized around major effects on the phase behavior, such as the effect of solvent, polyolefin size, and antisolvent (ethylene).

Solvent has an appreciable effect on the phase behavior of the system. As shown in Figure 2 for PEP790 mixtures, 1-butene shifts the LCST phase boundary to lower pressures (by approximately 100 bar) and to higher temperatures, compared to propylene. 1-Butene has a higher density than propylene and is a larger molecule. Thus, it is a better solvent than propylene. The mixture VL curve, for both systems, coincides with the solvent vapor pressure curve because addition of the polymer has a small effect on the bubble pressure of the mixture. A qualitative difference between the two systems is that, for the propylene + PEP790, a VLL line is observed, in contrast to the 1-butene + PEP790 mixture. SAFT predicts the phase behavior of these systems with $k_{ij} = 0$. Since the LCST for these systems is entropically driven, one concludes that SAFT correctly predicts the entropy of mixing for components that differ considerably in size. SAFT slightly overpredicts the critical point of the solvent which is typical of the noncubic equations of state.[41] In addition, SAFT predicts a small VLL region for the 1-butene + PEP790

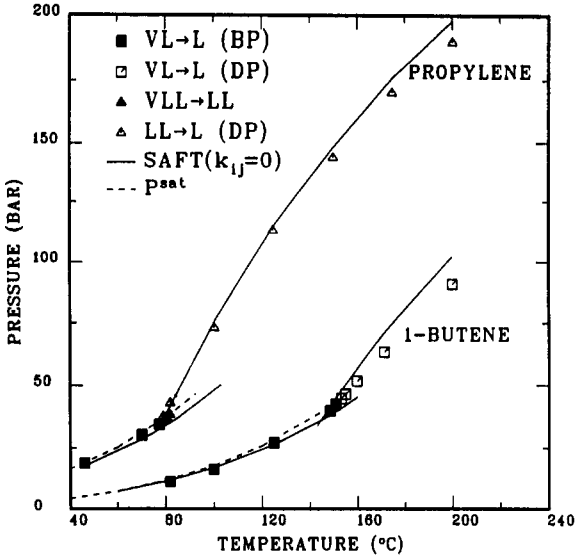

Figure 2. Experimental data[16] and theoretical predictions (k_{ij} = 0) for PEP790 + propylene and PEP790 + 1-butene. SAFT predicts quantitatively the various types of phase transitions. SAFT predicts a small VLL region for the PEP790 + 1-butene system that is not observed experimentally. In addition, SAFT slightly overpredicts the critical point of the solvent. The LL to L phase boundary is also referred to as LCST in the text.

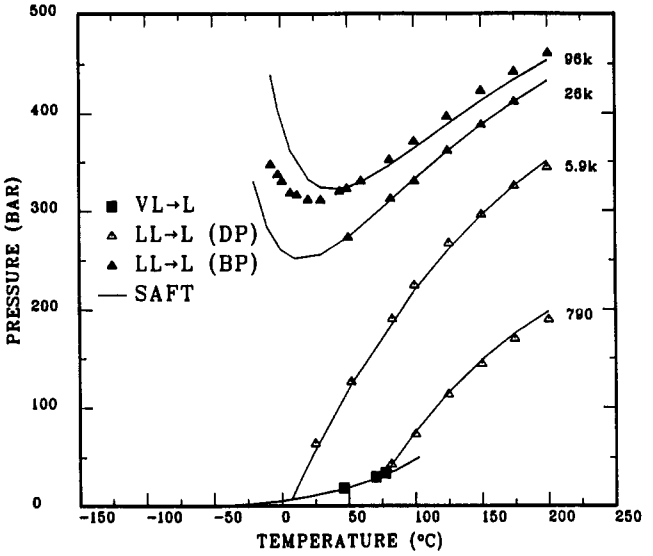

Figure 3. Experimental[16] and theoretical P–T phase boundaries for PEP + propylene for different PEP molecular weights. A molecular weight dependent binary interaction parameter, k_{ij}, is needed to correlate the phase behavior quantitatively. As the molecular weight of the polymer increases the phase boundary shifts to higher pressures, and finally the UCST and LCST curves merge.

which is not observed experimentally. However, the SAFT predictive power for these systems is far better than that of the Flory–Patterson approach.[16]

As the molecular weight of the polymer increases, the LCST curve shifts to lower temperatures and higher pressures, as shown in Figure 3 for propylene + PEPs having different molecular weights. The region of complete miscibility (above the LCST boundary) shrinks, and eventually the LCST and UCST curves merge for propylene + PEP96k into a U-LCST curve. In addition, for PEP790 and PEP5.9k, a dew-point-like phase transition is observed, whereas for PEP26k and PEP96k the phase transition is of the bubble-point type. While SAFT correctly predicts the U-LCST minimum for PEP96k, it is somewhat off in predicting the slope of the UCST branch of this curve. In addition, it predicts a U-LCST minimum

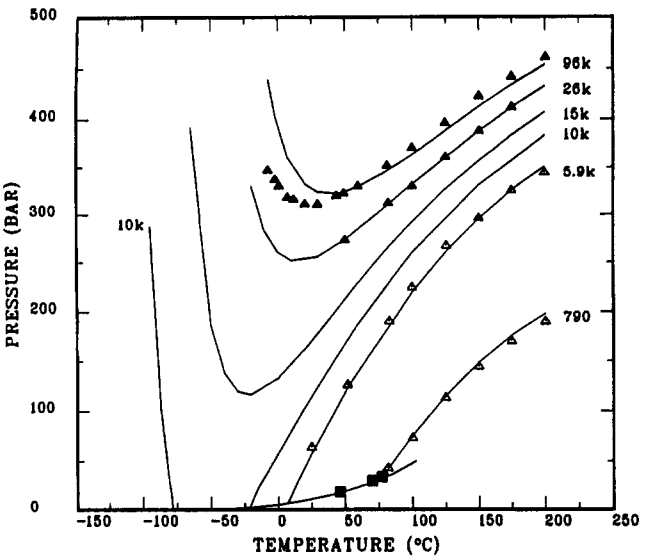

Figure 4. Experimental[16] and theoretical P–T phase boundaries for PEP + propylene for different PEP molecular weights. Using the binary interaction parameter correlation developed for this system, theoretical calculations are shown for various PEP molecular weights. For the PEP10k + propylene system, SAFT predicts a steep UCST curve with a UCEP around −80 °C.

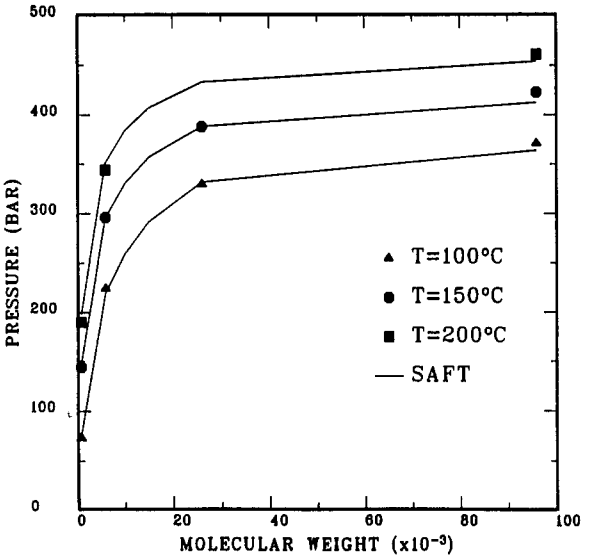

Figure 5. LCST pressure dependence on the polymer molecular weight for PEP + propylene at various temperatures from experimental data[16] and SAFT calculations.

for the PEP26k mixture at approximately 10 °C. The U-LCST behavior for PEP26k is later confirmed in a separate glass tube experiment.[16]

SAFT can correlate the experimental data shown in Figure 3 with the use of one binary parameter k_{ij} that depends on, and can be correlated against, the polymer molecular weight. The k_{ij} correlations used in this work are shown in Table IV.

These k_{ij} correlations allow for theoretical predictions where no experimental data are available, e.g., for propylene + PEP10k and propylene + PEP15k, as shown in Figure 4. The purpose for these calculations is to explore the UCST demixing, which cannot be observed experimentally because of low-temperature equipment limitations, and to quantify the molecular weight dependence of the U-LCST minimum. For propylene + PEP10k, SAFT predicts a separate UCST curve with an UCEP (upper critical end point) at approximately −80 °C. As shown in Figure 4, SAFT can predict a transition from separate UCST and LCST curves (propylene + PEP10k)

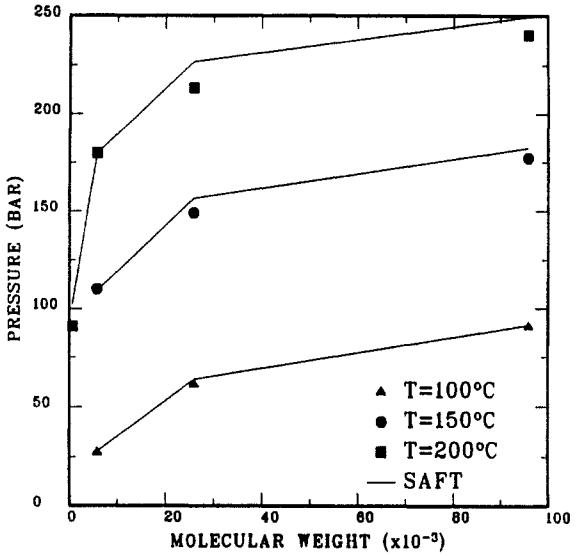

Figure 6. LCST pressure dependence on the polymer molecular weight for PEP + 1-butene at various temperatures from experimental data[16] and SAFT calculations.

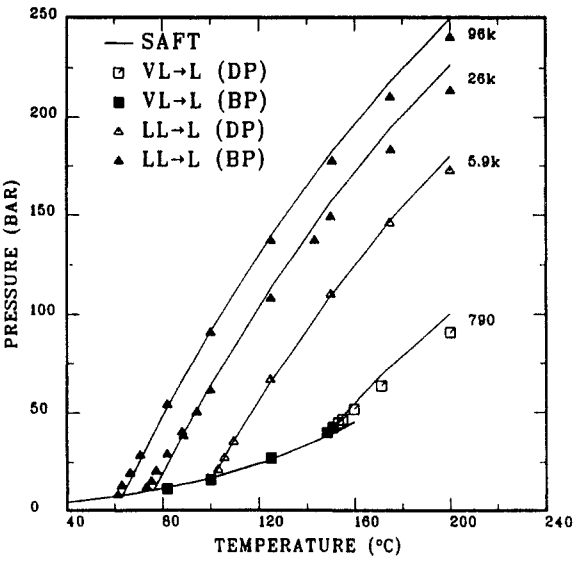

Figure 7. Experimental[16] and theoretical P–T phase boundaries for PEP + 1-butene for different PEP molecular weights. A molecular weight dependent binary interaction parameter, k_{ij}, is needed to correlate the phase behavior quantitatively.

to a single U-LCST curve (propylene + PEP15k) upon increasing the polymer molecular weight. Furthermore, increasing the polymer molecular weight increases the temperature and pressure of the U-LCST minimum, as shown in Figure 4 and Table V.

It should be mentioned that SAFT calculations become extremely sensitive to small changes in k_{ij} for high molecular weight polymers. For example, for the propylene + PEP96k system, the k_{ij} correlation gives a value of 0.027. If one sets $k_{ij} = 0$, then SAFT predicts that the LCST curve extends all the way to the vapor pressure curve. Such high sensitivity to small changes in k_{ij} was also observed by Liu and Prausnitz,[26] who used the PHCT equation of state.

The effect of the polymer molecular weight on the propylene + PEP LCST pressure is shown at three different temperatures in Figure 5. The LCST pressure is very sensitive to the polymer molecular weight below 30 000 and, especially, below 20 000. For higher molecular weights, however, the LCST pressure is very weakly dependent on the polymer molecular weight. A similar molecular weight dependence of the LCST pressure is

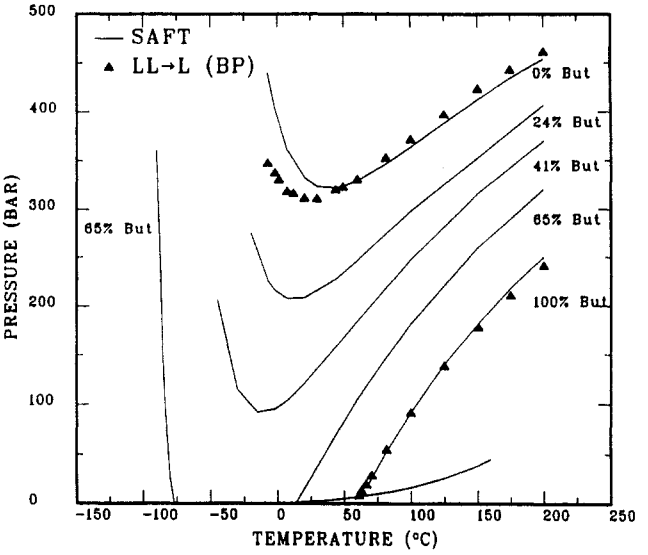

Figure 8. Experimental[16] and theoretical P–T phase boundaries for PEP96k + propylene + 1-butene. In the absence of 1-butene, the UCST and LCST curves merge. As the 1-butene concentration increases, the LCST boundary shifts to lower pressures and higher temperatures. For 65 wt % 1-butene in the system, separate UCST and LCST curves are predicted.

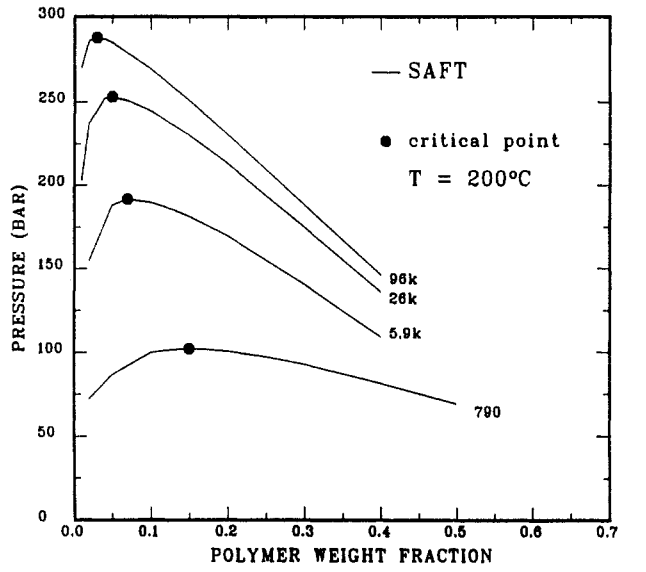

Figure 9. SAFT-calculated P–x phase diagrams for the PEP + 1-butene system at 200 °C. The phase boundary shifts to higher pressure and the calculated critical point to lower polymer composition for higher molecular weight polymers.

observed for 1-butene + PEP in Figure 6, where the LCST pressure is shown at the same three temperatures as in Figure 5.

However, in general, the phase behavior of the 1-butene + PEP system is qualitatively different from that of the propylene + PEP system, at least for the high molecular weight polymers, as shown in Figure 7. For all the systems examined, the LCST curve intersects with the vapor pressure curve, and no U-LCST type of phase behavior is detected. As for propylene, increasing the polymer molecular weight decreases the one-phase region. In other words, the LCST boundaries are shifted to lower temperatures and higher pressures. SAFT results are in a very good agreement with the experimental data. As for propylene, only one molecular weight dependent binary parameter (k_{ij} given in Table 4) is used.

This binary parameter, derived from the experimental data for propylene + PEP and 1-butene + PEP binary systems, without further readjustment, is also used to

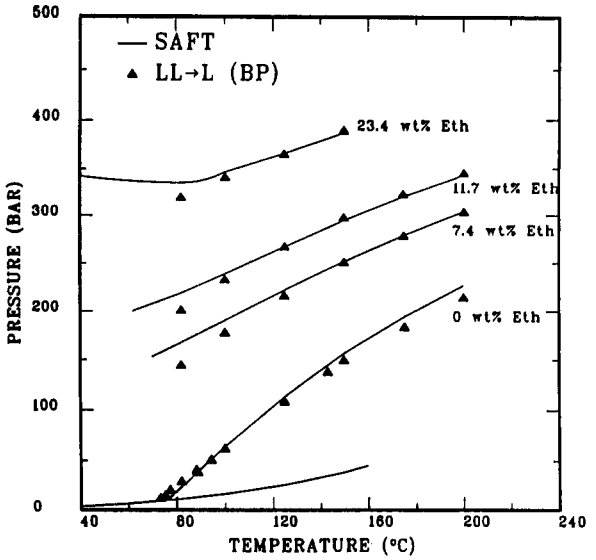

Figure 10. Experimental and theoretical P–T phase boundaries for PEP26k + 1-butene + ethylene at different ethylene concentrations. For 23.4 wt % ethylene in the mixture, SAFT predicts that the UCST and LCST merge.

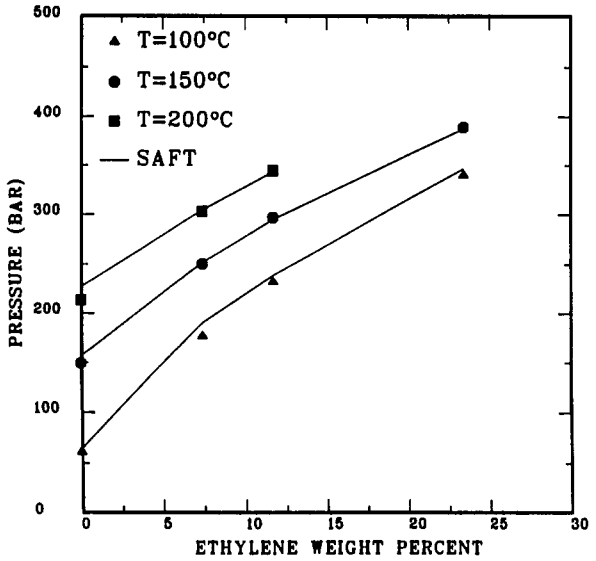

Figure 11. LCST pressure for PEP26k + 1-butene + ethylene dependence on the ethylene concentration at constant temperature. Experimental data and SAFT calculations.

predict the phase behavior of the ternary propylene + 1-butene + PEP96k system, shown in Figure 8. In all the cases, the polymer composition is 15 wt %. In the absence of 1-butene in the system, i.e., for propylene + PEP96k, the U-LCST phase behavior is observed. As the 1-butene concentration increases, the binary solvent becomes a "better" solvent because 1-butene acts like a cosolvent. As a result, the one-phase region increases (the LCST phase boundary shifts to lower pressures and higher temperatures). Eventually, for a solvent containing 65 wt % 1-butene (on a polymer-free basis), SAFT predicts that the U-LCST curve splits and that the separate UCST and LCST curves intersect with the vapor pressure curve.

While the scope of this work is limited to the systems having a constant polymer concentration (around 15 wt %), we make an attempt to predict an LCST dependence on the polymer concentration in 1-butene solutions. Figure 9 illustrates a preliminary, SAFT-generated P–x phase diagram for 1-butene + PEP at 200 °C. As the polymer molecular weight increases, the phase boundary shifts to higher pressures, and thus the two-phase region (of limited miscibility) increases. In addition, the calculated critical

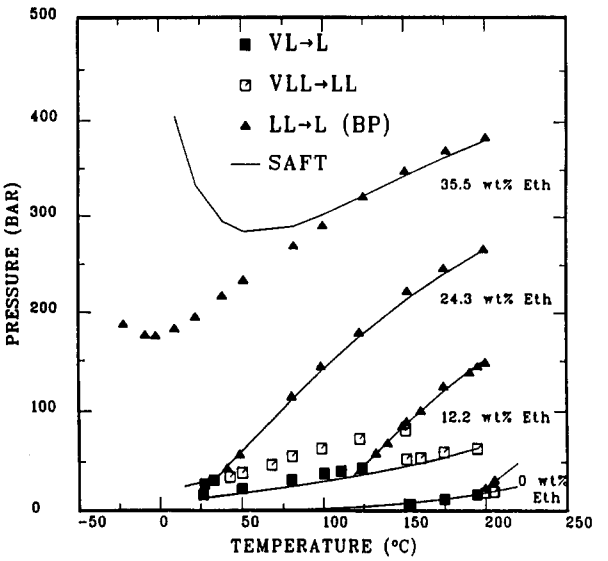

Figure 12. Experimental and theoretical P–T phase boundaries for PEP26k + 1-hexene + ethylene at different ethylene concentrations. The binary parameter, k_{PE}, used for these calculations is the same as that used for the PEP26k + 1-butene + ethylene system shown in Figure 10.

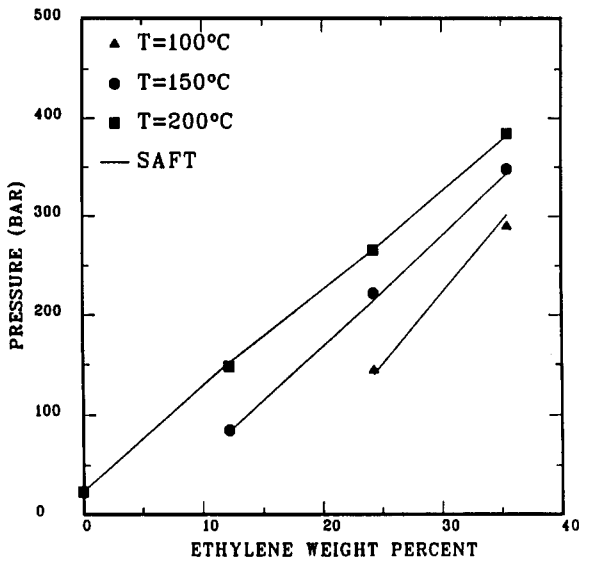

Figure 13. LCST pressure for PEP26k + 1-butene + ethylene dependence on the ethylene concentration at constant temperature. Experimental data and SAFT calculations.

Table IV
SAFT k_{ij} Correlation[a]

system	$A^{(1)}$	$A^{(2)}$	$A^{(3)}$
PEP + propylene	0.027	−0.02209	1.034×10^{-4}
PEP + 1-butene	0.005	−0.03499	7.483×10^{-5}
PEP67k + *n*-hexane	−0.02	0.0	0.0
n-hexane + propylene	0.063	0.0	0.0

[a] $k_{ij} = A^{(1)} + A^{(2)} \exp(-A^{(3)}M_P)$. M_P = PEP molecular weight in g/mol.

point (filled circle) shifts to lower polymer compositions upon increasing the polymer molecular weight. These trends are qualitatively correct. However, our preliminary experimental data suggest that the predicted P–x curves should be more flat. This issue is being addressed in our current work.

In a ternary system of 1-butene + ethylene + PEP26k, ethylene acts like a powerful antisolvent because it drastically reduces the 1-butene + PEP26k density, which is shown in Figure 10. As the ethylene concentration (polymer-free basis) increases, the phase boundary shifts

Table V
SAFT-Calculated U-LCST Minima for the PEP + Propylene System

PEPMW	T_{min} (°C)	P_{min} (bar)
96k	44.0	322.2
26k	10.0	251.8
15k	-20.0	116.4
≤10k	U-LCST minimum reaches the VLL curve	

to higher pressures. For example, addition of 7.4 wt % ethylene to the system shifts the LCST by more than 80 bar. A further increase of the ethylene concentration to 23.4 wt % results in a U-LCST-type of behavior, as predicted by SAFT at 23.4 wt %. No experimental data are available below 80 °C to verify these predictions. The effect of the ethylene weight percent on the cloud-point pressure is shown in Figure 11 at three different temperatures. For example, addition of about 10 wt % ethylene can increase the cloud-point pressure by as much as 100 bar. SAFT results are in excellent agreement with the experimental data.

An ethylene antisolvent effect is also observed for the ethylene + 1-hexene + PEP26k system, as shown in Figure 12 for 0, 12.2, 24.3, and 35.5 wt % ethylene (polymer-free basis). Increasing the ethylene weight fraction shifts the LCST boundary to higher pressures and lower temperatures and, hence, decreases the region of complete miscibility. Furthermore, for 35.5 wt % ethylene (polymer-free basis), the UCST and LCST curves merge into a single U-LCST curve.

SAFT quantitatively correlates the LCST curves up to 24.3 wt % using two adjustable parameters, k_{EP} (ethylene + PEP26k) and k_{HP} (1-hexene + PEP26k). However, the k_{EP} is determined based on the 1-butene + ethylene + PEP26k data (Figure 10). Hence, only one parameter, k_{HP}, is fitted to the experimental data presented in Figure 12. For the case of 35.5 wt % ethylene, SAFT correctly predicts the existence of a U-LCST curve but overpredicts the minimum pressure point. This can be attributed to the ethylene molecular parameters derived at much lower temperatures, as discussed above. The effect of the ethylene weight percent on the LCST pressure is shown in Figure 13 at three different temperatures. SAFT calculations are in excellent agreement with the experimental data.

Up to this point, we have been concerned with binary and ternary systems with a nearly monodisperse polymeric component. In order to extend SAFT to multicomponent systems and to polydisperse components, we use experimental data obtained for a quaternary mixture of *n*-hexane (1) + methylcyclopentane (2) + SCF (3) + PEP67k (4) by McHugh and Guckes[17] where the SCF is either propylene or ethylene. PEP67k has a number-average molecular weight of 67 000 and a polydispersity of $\bar{M}_w/\bar{M}_n$ = 2.2. However, in our phase equilibrium calculations PEP67k is treated as a monodisperse component. This is because, we find that, the bubble-point-like transitions in this M_w range and at a constant polymer concentration are relatively insensitive to polydispersity. For these systems, the concentration of polymer in the solvent (SCF-free basis) is 5.24 wt %. In addition, the organic solvent contains 88 wt % *n*-hexane, 9.5 wt % methylcyclopentane, and 2.5 wt % 3-methylpentane. 3-Methylpentane is ignored in the calculations.

The phase diagram for the *n*-hexane (1) + methylcyclopentane (2) + propylene (3) + PEP67k (4) system is shown in Figure 14 for two different propylene concentrations (overall basis). In order to correlate the VL, LL, and VLL phase equilibria shown in Figure 14, we need

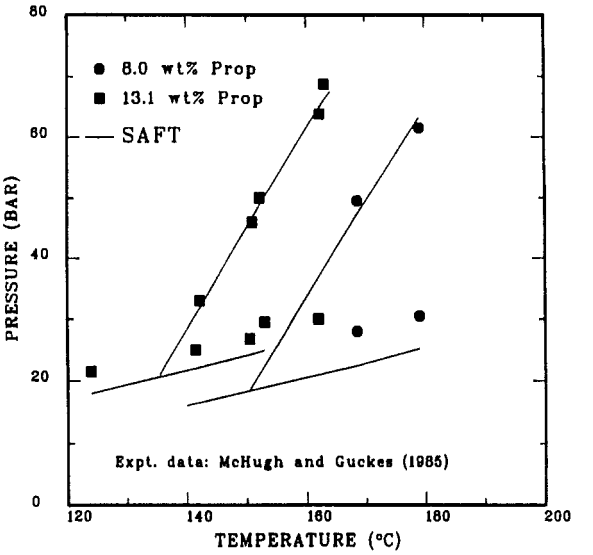

Figure 14. Experimental[17] and SAFT *P–T* phase boundaries for *n*-hexane + methylcyclopentane + propylene + PEP67k at constant propylene concentration. Three temperature-independent binary interaction parameters, k_{ij}, are needed to correlate the phase behavior quantitatively. Propylene concentrations are on a total basis.

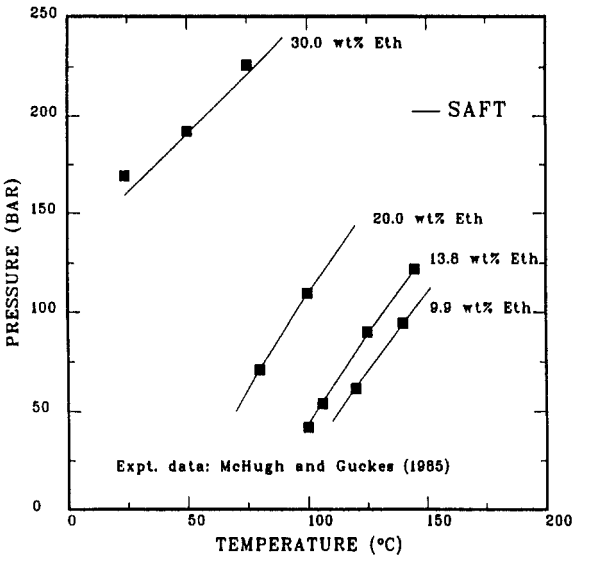

Figure 15. Experimental[17] and SAFT *P–T* phase boundaries for *n*-hexane + methylcyclopentane + ethylene + PEP67k at constant ethylene concentrations. Two binary interaction parameters, k_{ij}, are needed to correlate the phase behavior quantitatively. Ethylene concentrations are on a total basis.

three binary parameters, $k_{hexane-propylene}$, $k_{hexane-PEP}$, and $k_{propylene-PEP}$. $k_{propylene-PEP}$ is calculated from the generalized correlation given in Table IV and derived from the propylene + PEP data (Figure 3). $k_{hexane-propylene}$ and $k_{hexane-PEP}$ are fitted to the quaternary data (Figure 14). As expected, the $k_{hexane-propylene}$ parameter controls the VL and VLL curves and, in principle, could have been derived from *n*-hexane + propylene VLE data. On the other hand, $k_{hexane-PEP}$ is found to control the LCST curve. It is worth noting that both parameters are molecular weight independent and have a constant value given in Table IV.

Finally, the phase diagram for the quaternary mixture containing ethylene is shown in Figure 15 at constant ethylene concentrations. SAFT accurately correlates the LCST curves with the use of two binary parameters, $k_{hexane-PEP}$ and $k_{ethylene-PEP}$. $k_{hexane-PEP}$ is fitted to the experimental data in Figure 14, as discussed in the previous paragraph, whereas $k_{ethylene-PEP}$ is fitted to the experimental data in Figure 15.

In the three ternary phase diagrams for ethylene systems (Figures 10, 12, and 15), the phase boundary curves are calculated at constant ethylene concentration. Only in this case, we are limited to using SAFT at a constant ethylene concentration because the k_{ij} binary parameter for ethylene–PEP, unfortunately, varies with ethylene concentration.

In general, k_{ij} concentration dependence is inconsistent with the mixing rules (eqs 7–11) because it introduces an additional concentration dependence that is not accounted for by the chemical potential expression. One possible reason for this concentration dependence of k_{ij} is that the mixing rules used here are not adequate for the ethylene ternaries. Hence, to be consistent, we use SAFT at a constant ethylene concentration only. However, in all the other cases discussed in this work, k_{ij} is composition-independent.

5. Conclusions

A combination of a high-pressure experiment (variable-volume optical cell) and molecular theory (statistical associating fluid theory, SAFT) is used to quantify systematically the effects of pressure, temperature, composition, and polymer and solvent size on LCST, UCST, VL, and VLL transitions in binary, ternary, and quaternary olefin–polyolefin systems.

Supercritical ethylene is found to reduce drastically the mutual miscibility of 1-butene + PEP and 1-hexene + PEP and, hence, to increase the LCST pressures needed to maintain the ternary mixtures in a one-phase region. This ethylene antisolvent effect is modeled with SAFT.

SAFT polymer parameters can be estimated from simple generalized correlations based on molecular weight only, which are valid for amorphous polyolefins. For mixtures, SAFT requires one binary polymer–solvent interaction parameter, which is related to the dispersion energy. In general, this parameter is found to be dependent on the polymer molecular weight. Only for the ethylene systems, the vdW1 mixing rules are used at constant ethylene concentration.

SAFT predicts UCST curves and, upon increasing the size difference between the polymer and solvent, UCST–LCST merging into a single U-LCST curve. Furthermore, SAFT can simultaneously predict the LCST curves and the VL and VLL transitions. This has not been demonstrated before.

Acknowledgment. We are grateful to Lewis J. Fetters for sharing with us his poly(ethylene–propylene) samples and to John M. Prausnitz for comments that enhanced this paper. Stimulating and helpful discussions with Norbert Baron, Yee C. Chiew, Charles Cozewith, Bernard Folie, Christopher J. Gregg, and Jeffrey L. Hemmer are also gratefully acknowledged. Parts of this work were presented at the Annual Meeting of the American Institute of Chemical Engineers, Los Angeles, CA, 1991, and at the Sixth International Conference on Fluid Properties and Phase Equilibria, Cortina D'Ampezzo, Italy, 1992.

References and Notes

(1) Patterson, D. *Macromolecules* **1969**, *2*, 672.
(2) Stroeks, A.; Nies, E. *Macromolecules* **1990**, *23*, 4092.
(3) Walker, J. S.; Vause, C. A. *Sci. Am.* **1987**, *98* (5), 98.
(4) Sanchez, I. C.; Balazs, A. C. *Macromolecules* **1989**, *22*, 2325.
(5) Zeman, L.; Biros, J.; Delmas, G.; Patterson, D. *J. Phys. Chem.* **1972**, *76*, 1206.
(6) Shultz, A. R.; Flory, P. J. *J. Am. Chem. Soc.* **1952**, *74*, 4760.
(7) Flory, P. J.; Hocker, H. *Trans. Faraday Soc.* **1971**, *67*, 2258.
(8) Zeman, L.; Patterson, D. *J. Phys. Chem.* **1972**, *76*, 1214.
(9) Siow, K. S.; Delmas, G.; Patterson, D. *Macromolecules* **1972**, *5*, 29.
(10) Saeki, S.; Kuwahara, N.; Konno, S.; Kaneko, M. *Macromolecules* **1973**, *6*, 246.
(11) Saeki, S.; Kuwahara, N.; Nakata, M.; Kaneko, M. *Polymer* **1975**, *16*, 445.
(12) Cowie, J. M. G.; McEwen, I. J. *Polymer* **1983**, *24*, 1445.
(13) Bae, Y. C.; Lambert, S. M.; Soane, D. S.; Prausnitz, J. M. *Macromolecules* **1991**, *24*, 4403.
(14) Ehrlich, P. *J. Polym. Sci., Part A* **1965**, *3*, 131.
(15) de Loos, T. W.; Poot, W.; Diepen, A. M. *Macromolecules* **1983**, *16*, 111.
(16) Chen, S.-J.; Radosz, M. *Macromolecules* **1992**, *25*, 3089.
(17) McHugh, M. A.; Guckes, T. L. *Macromolecules* **1985**, *18*, 674.
(18) Seckner, A. J.; McClellan, A. K.; McHugh, M. A. *AIChE J.* **1988**, *34*, 9.
(19) Meilchen, M. A.; Hasch, B. M.; McHugh, M. A. *Macromolecules* **1991**, *24*, 4874.
(20) McHugh, M. A.; Krukonis, V. J. *Supercritical Fluid Extraction: Principles and Practice*; Butterworths: Boston, MA, 1986.
(21) Flory, P. J. *Principles of Polymer Chemistry*; Cornell University Press: Ithaca, NY, 1953.
(22) Qian, C.; Mumby, S. J.; Eichinger, B. E. *Macromolecules* **1991**, *24*, 1655.
(23) Flory, P. J.; Orwoll, R. A.; Vrij, A. *J. Am. Chem. Soc.* **1964**, *86*, 3507.
(24) Walsh, D. J.; Dee, G. T.; Halary, J. L.; Ubiche, J. M.; Millequant, M.; Lesec, J.; Monnerie, L. *Macromolecules* **1989**, *22*, 3395.
(25) Ougizawa, T.; Dee, G. T.; Walsh, D. J. *Macromolecules* **1991**, *24*, 3834.
(26) Liu, D. D.; Prausnitz, J. M. *Macromolecules* **1979**, *12* 454.
(27) Liu, D. D.; Prausnitz, J. M. *Ind. Eng. Chem. Process Des. Dev.* **1980**, *19*, 205.
(28) Sanchez, I. C.; Lacombe, R. H. *J. Phys. Chem.* **1976**, *80*, 2352.
(29) Chapman, W. G.; Gubbins, K. E.; Jackson, G.; Radosz, M. *Ind. Eng. Chem. Res.* **1990**, *29*, 1709.
(30) Huang, S. H.; Radosz, M. *Ind. Eng. Chem. Res.* **1990**, *29*, 2284.
(31) Huang, S. H.; Radosz, M. *Ind. Eng. Chem. Res.* **1991**, *30*, 1994.
(32) Mays, J.; Hadjichristidis, N.; Fetters, L. J. *Macromolecules* **1984**, *17*, 2723.
(33) Wertheim, M. S. *J. Stat. Phys.* **1984**, *35*, 35.
(34) Wertheim, M. S. *J. Stat. Phys.* **1986**, *42*, 459.
(35) Wertheim, M. S. *J. Stat. Phys.* **1986**, *42*, 477.
(36) Carnahan, N. F.; Starling, K. E. *J. Chem. Phys.* **1969**, *51*, 635.
(37) Mansoori, G. A.; Carnahan, N. F.; Starling, K. E.; Leland, T. W. *J. Chem. Phys.* **1971**, *54*, 1523.
(38) Alder, B. J.; Young, D. A.; Mark, M. A. *J. Chem. Phys.* **1972**, *56*, 3013.
(39) Chen, S. S.; Kreglewski, A. *Ber. Bunsen-Ges. Phys. Chem.* **1977**, *81*, 1048.
(40) Walas, S. M. *Phase Equilibria in Chemical Engineering*; Butterworths: Stoneham, MA, 1985.
(41) Gregorowicz, J.; Fermeglia, M.; Soave, G.; Kikic, I. *Chem. Eng. Sci.* **1991**, *46*, 1427.